ORGANOMETALLICS

pubs.acs.org/Organometallics Article

# Scope and Mechanism of the Ruthenium-Catalyzed $sp^3$ C−H Coupling Reaction of 2-Alkylindoles with Enones for the Synthesis of Carbazole Derivatives

Krishna Prasad Gnyawali, Mina Son, Donghun Hwang, Nuwan Pannilawithana, Mu-Hyun Baik,* and Chae S. Yi*

Cite This: *Organometallics* 2025, 44, 325−334 Read Online

ACCESS | Metrics & More | Article Recommendations | Supporting Information



**ABSTRACT:** The catalytic system consisting of a cationic Ru−H complex **1** and 3,4,5,6-tetrachloro-1,2-benzoquinone (**L1**) was found to be highly effective for the dehydrative $sp^3$ C−H coupling reaction of 2-alkyl substituted indoles with enones to form 2,4-disubstituted carbazole products. The analogous coupling reaction of 2-alkylindoles with linear enones bearing the cyclic olefinic group afforded tetracyclic carbazole products. A normal deuterium kinetic isotope effect was measured from the coupling reaction of 1,2-dimethylindole versus 1-methyl-2-(methyl-$d_3$)indole with (*E*)-3-penten-2-one ($k_H/k_D$ = 2.5). The Hammett plot was constructed from the reaction of *para*-substituted indoles 5-X-1,2-dimethylindole (X = OMe, Me, H, F, and Cl) with 4-phenyl-3-buten-2-one ($\rho$ = −1.6 ± 0.2). The density functional theory (DFT) calculations were performed to obtain a complete energy profile for the coupling reaction. The combined experimental and DFT computational data revealed a detailed mechanistic path that features an initial coupling of indole and enone substrates, the turnover-limiting heterolytic $sp^3$ C−H activation step, and the subsequent cyclization and dehydration steps. The catalytic method provides an efficient synthesis of carbazole derivatives from the dehydrative $sp^3$ C−H coupling reaction of readily available indole with enone substrates without employing any reactive reagents or forming wasteful byproducts.

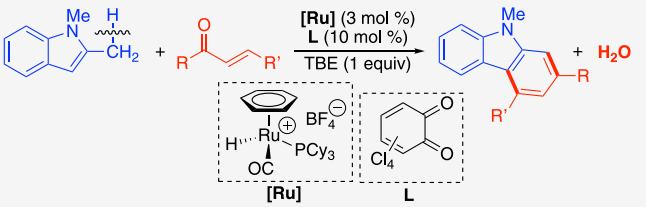


## INTRODUCTION

Transition metal-catalyzed C−C coupling methods through $sp^2$ C−H bond activation of unsaturated hydrocarbon substrates have emerged as one of the most powerful protocols in organic synthesis.[1] Over the last few decades, extensive research has led to the development of highly selective catalytic C−C coupling methods through $sp^2$ C−H bond activation, enabling the step-efficient synthesis of a variety of complex organic molecules of pharmacological importance.[2] In contrast, catalytic C−C coupling methods via $sp^3$ C−H bond activation of saturated hydrocarbon substrates still remain as the frontier topic in C−H functionalization research. Among the many innovative strategies for catalytic $sp^3$ C−H activation methods, heteroatom-directed chelate assistance approach has proven to be highly effective in achieving site-selective $sp^3$ C−H coupling reactions for saturated hydrocarbon derivatives.[3] In a pioneering work, Jun and co-workers introduced metal−ligand cooperative bifunctional catalysis protocols, which have become valuable tools for direct $sp^3$ C−H alkylation and related coupling reactions of saturated hydrocarbon substrates bearing carbonyl and nitrogen chelate groups.[4] Chen and co-workers devised highly efficient Pd-catalyzed $sp^3$ C−H alkylation protocols to derivatize $\alpha$-amino acid substrates.[5] Additionally, catalytic cross-dehydrogenative coupling methods between two different $sp^3$ C−H bonds have been shown to be a versatile C−C bond formation strategy.[6] A variety of regioselective $sp^3$ C−H alkylation and related C−C bond-forming reactions of saturated amines and carbonyl compounds have been successfully utilized for the late-stage functionalization of biologically active molecules.[7] In a series of seminal reports, Yu and co-workers developed a range of site-selective $sp^3$ C−H arylation and other C−C coupling methods by using transient nitrogen directing groups.[8] Recently, photocatalytic proton-coupled hydrogen atom transfer technologies have been successfully devised for chemoselective $sp^3$ C−H alkylation and other C−X bond-forming reactions.[9] A variety of inorganic/organometallic and organic-based photoredox catalytic systems have been extensively explored for both $sp^2$ and $sp^3$ C−H functionalization methods.[10] Despite these rapidly expanding advances, the development of broadly applicable catalytic C−C coupling methods via $sp^3$ C−H

**Received:** November 7, 2024
**Revised:** December 4, 2024
**Accepted:** December 6, 2024
**Published:** December 19, 2024

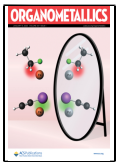





https://doi.org/10.1021/acs.organomet.4c00470
*Organometallics* 2025, 44, 325−334

Scheme 1. $sp^3$ C−H Coupling vs C−C Cleavage Reaction for the Coupling Reaction of 1,2-Dimethylindole with an Enone

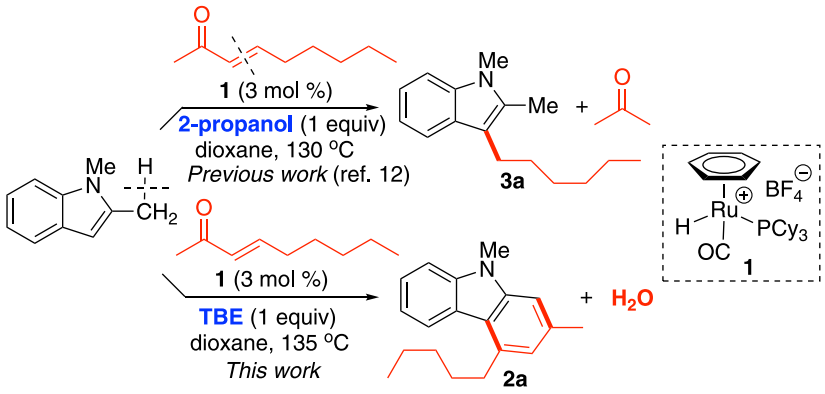


Table 1. Catalyst and Additive Screening for the Coupling of 1,2-Dimethylindole with (*E*)-3-Nonen-2-One[a]

| entry | catalyst | deviation from standard conditions | 2a:3a (%)[b] |
|---|---|---|---|
| 1 | **1** | none | 82:12 |
| 2 | **1** | without TBE | 68:15 |
| 3 | **1** | without **L1** | 50:13 |
| 4[c] | **1** | with 2-propanol (0.5 mmol) | 6:81 |
| 5 | **1** | in dichloroethane | 41:22 |
| 6 | **1** | in toluene | 22:18 |
| 7 | $[(PCy_3)_2(CO)(CH_3CN)_2RuH]^+BF_4^-$ | | 43:13 |
| 8 | $[(PCy_3)(CO)RuH]_4(O)(OH)_2/HBF_4{\cdot}OEt_2$ | | 26:4 |
| 9 | $(PCy_3)_2(CO)RuHCl/HBF_4{\cdot}OEt_2$ | | 20:4 |
| 10 | $RuCl_2(PPh_3)_3/HBF_4{\cdot}OEt_2$ | | 12:6 |
| 11 | $Ru_3(CO)_{12}/HBF_4{\cdot}OEt_2$ | | 8:6 |
| 12 | $[(COD)RuCl_2]_x/HBF_4{\cdot}OEt_2$ | | 10:5 |
| 13 | $PCy_3/HBF_4{\cdot}OEt_2$ | | 0 |
| 14 | $AlCl_3$ | | 0 |
| 15 | $HBF_4{\cdot}OEt_2$ | | 0 |

[a]Standard conditions: 1,2-dimethylindole (0.5 mmol), (*E*)-3-nonen-2-one (0.6 mmol), catalyst (3 mol %), **L1** (10 mol %), TBE (0.5 mmol) 1,4-dioxane (2 mL), 135 °C, 24 h. [b]The product yield was determined by GC−MS by using hexamethylbenzene as an internal standard. TBE = *t*-butylethylene, **L1** = 3,4,5,6-tetrachloro-1,2-benzoquinone. [c]In dichloroethane.

activation for the synthesis of complex organic molecules remains a challenging goal in the catalysis field of research.

We previously developed a number of catalytic dehydrative $sp^2$ C−H coupling methods of phenols with carbonyl compounds, which have led to efficient formation of various synthetically valuable oxygen heterocycles while forming water as the only byproduct.[11] As part of our ongoing efforts to design new sustainable coupling methods, we have been searching for new catalytic C−C coupling protocols via $sp^3$ C−H activation, which are suitable for late-stage functionalization of biologically active saturated hydrocarbon compounds under environmentally sustainable conditions. Herein, we report a highly efficient synthesis of carbazole derivatives through the dehydrative $sp^3$ C−H coupling reaction of 2-alkylindoles with enone compounds. The catalytic coupling method employs readily available starting materials to form 2,4-disubstituted carbazole derivatives that are not readily synthesized by other traditional methods.

## RESULTS AND DISCUSSION

**Reaction Discovery and Substrate Scope.** While exploring new strategies for chelate-assisted dehydrative coupling methods, we previously discovered that the coupling reaction of 1,2-dimethylindole with linear enones in the presence of a hydrogen source (2-propanol) led to the regioselective C−C bond cleavage of the enone substrate in forming the indole coupling products (Scheme 1).[12] Recognizing that a hydrogen rich environment might have facilitated the C−C cleavage reaction, we performed the same coupling reaction under a hydrogen-deficient condition. Thus, the treatment of 1,2-dimethylindole with (*E*)-3-nonen-2-one in the presence of the Ru−H catalyst $[(C_6H_6)(PCy_3)(CO)RuH]^+BF_4^-$ (**1**) and a hydrogen scavenger *t*-butylethylene (1 equiv) predominantly formed the carbazole product **2a** with less than 20% of the C−C bond cleavage product **3a** in a crude mixture. Encouraged by the initial results, wherein both $sp^2$ and $sp^3$ C−H bond cleavages on the indole substrate have been achieved in forming the carbazole product **2a**, we sought to establish an optimized reaction condition for the formation of carbazole product **2a**. In light of the recent discoveries on the promotional effect of benzoquinone ligands,[12,13] both Ru catalysts as well as catechol and benzoquinone additives were extensively screened for the coupling reaction of 1,2-dimethylindole with (*E*)-3-nonen-2-one (Table S1, Supporting Information). The cationic Ru−H complex **1** with 3,4,5,6-tetrachloro-1,2-benzoquinone (**L1**) was found to be the most effective in selectively forming product **2a** among the screened catalysts and additives (Table 1), and the addition of a hydrogen scavenger further improved the selectivity of carbazole product **2a** (entry 2). We eventually established


https://doi.org/10.1021/acs.organomet.4c00470
Organometallics 2025, 44, 325−334

Table 2. Synthesis of Carbazoles from the $sp^3$ C−H Coupling Reaction of 2-Alkylindoles with Enones[a,b]

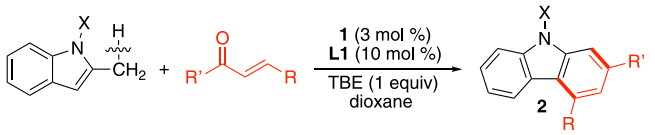


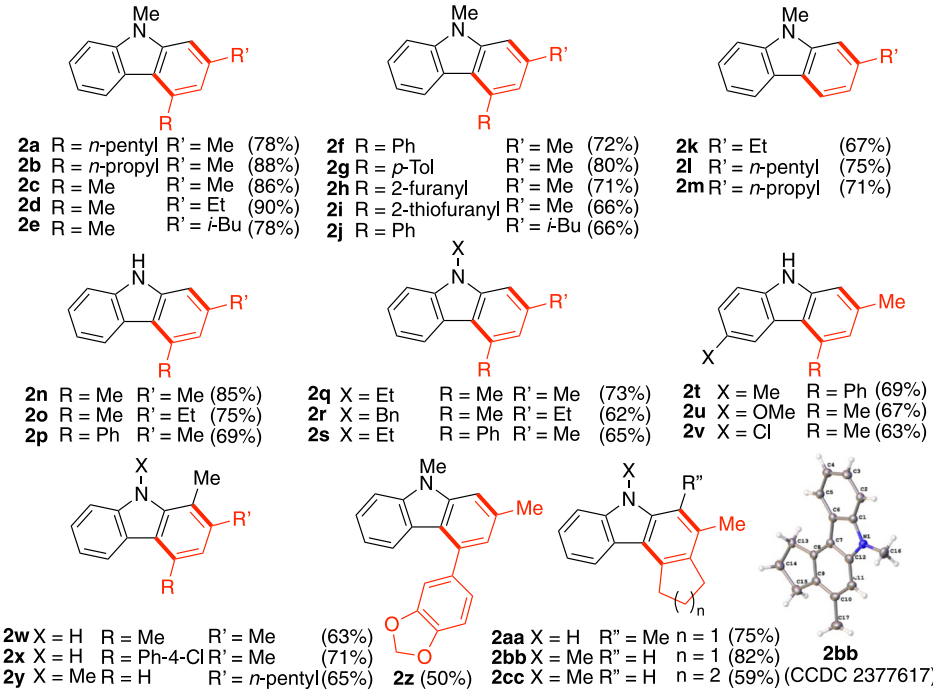


[a]Reaction conditions: indole (0.50 mmol), enone (0.60 mmol), *t*-butylethylene (0.50 mmol), **1** (3 mol %), **L1** (10 mol %), 1,4-dioxane (2 mL), 135 °C, 24 h. [b]Isolated yields.

the standard conditions for the formation of carbazole product **2a** over the C−C bond cleavage product **3a**, which consisted of the catalytic system of **1** (3 mol %)/**L1** (10 mol %) and *t*-butylethylene (1 equiv) as the hydrogen scavenger in 1,4-dioxane solution (entry 1).

We explored the substrate scope for the coupling reaction by using the standard conditions established in Table 1 (Table 2). The coupling reaction of 1,2-dimethylindole with both aliphatic- and aryl-substituted enones proceeded smoothly to form the carbazole products **2a**−**j**. The coupling with enones bearing a terminal olefinic group selectively led to the 2-substituted carbazole products **2k**−**m**. The coupling of both unprotected 2-methylindole and *N*-protected 2-methylindoles with linear enones formed the 2,4-disubstituted carbazole products **2n**−**p**, **2t**−**v**, and **2q**−**s**, respectively. The analogous coupling reaction of 2-ethylindole with linear enones formed 1,2,4-trisubstituted carbazole products **2w**−**y**. The coupling of 1,2-dimethylindole with (*E*)-4-(benzo[*d*][1,3]dioxol-5-yl)but-3-en-2-one formed the 2,4-disubstituted carbazole product **2z**, while the coupling with the enones bearing a cyclic olefinic group afforded the tetracyclic carbazole products **2aa**−**cc**. To demonstrate synthetic utility, we performed a preparatory scale reaction of 1,2-dimethylindole (3.0 mmol) with (*E*)-3-penten-2-one (3.6 mmol), which led to the isolation of coupling product **2c** in an 81% yield (0.51 g). Though the formation of C−C bond cleavage products **3** was detected in a crude reaction mixture in most cases (ca. 5−10%), analytically pure carbazole products **2** were readily obtained by column chromatography on silica gel, and their structures were completely established by spectroscopic methods. The molecular structure of **2bb** was unambiguously determined by X-ray crystallography.

**Combined Experimental and DFT Computational Mechanistic Study.** We examined the detailed mechanism of the coupling reaction of 1,2-dimethylindole with an enone substrate by employing combined experimental and computational methods. Considering the previously established results on the deaminative coupling reactions catalyzed by a Ru-catecholate species,[13,14] we hypothesized that a catalytically active Ru−H species would be initially formed from the ligand substitution reaction of **1** with the benzoquinone ligand **L1**. In an effort to detect catalytically relevant species, we monitored the coupling reaction of 1,2-dimethylindole with (*E*)-3-penten-2-one by using NMR spectroscopic techniques (Scheme 2). Thus, a stoichiometric mixture of complex **1** (0.10 mmol), 1,2-dimethylindole (0.10 mmol), (*E*)-3-penten-2-one (0.10 mmol), and 3,3-dimethyl-1-butene (0.10 mmol) in $CD_2Cl_2$ (0.5 mL) in a resealable NMR tube was immersed in an oil bath set at 125 °C, and the tube was taken out periodically to record the NMR spectrum at ambient temperature. After just 2 min of heating at 125 °C, four new sets of Ru−H signals rapidly appeared at $\delta$ −12.0 (d, $J_{PH}$ = 27.5 Hz), −12.1 (d, $J_{PH}$ = 27.4 Hz), −13.0 (d, $J_{PH}$ = 27.1 Hz), and −13.1 (d, $J_{PH}$ = 27.2 Hz) ppm in a 1:1:1.6:1.6 ratio, as monitored by $^1$H NMR, which were assigned to four diastereomeric mixtures of the arene-coordinated Ru−H complex **4** (Figure 1). The formation of free benzene molecule was also seen by $^1$H NMR. Upon further heating for 30 min, a new set of Ru−H


https://doi.org/10.1021/acs.organomet.4c00470
Organometallics 2025, 44, 325−334

**Scheme 2. Stoichiometric Reaction of 1 with 1,2-Dimethylindole and (*E*)-3-Nonen-2-One**

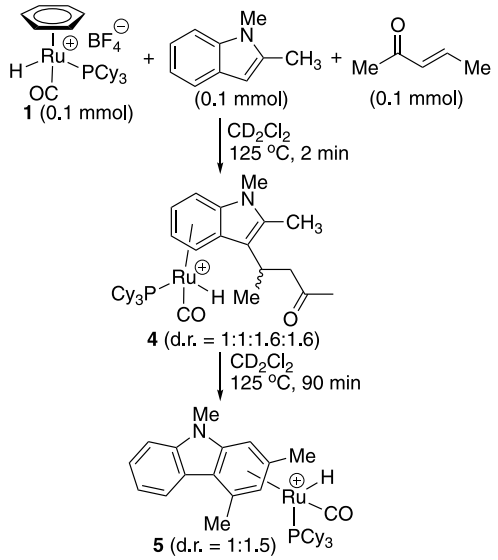


signals began to appear at $\delta$ −12.4 (d, $J_{PH}$ = 27.1 Hz) and −12.9 (d, $J_{PH}$ = 27.2 Hz) ppm at the expense of **4**, which were assigned to a diastereomeric mixture of the product-coordinated complex **5** (d.r. = 1:1.5). The Ru−H peaks for both **4** and **5** matched well with the signals formed independently from the treatment of **1** with the 2-methylindole substrate and product **2a**, respectively. The product-coordinated complex **5** eventually predominates at the expense of both **1** and **4** after heating at 125 °C for 90 min. Unfortunately, attempts to detect Ru−H signals from the analogous reaction mixture of **1** in the presence of the benzoquinone **L1** were not successful. We attribute this to rapid proton transfer to the oxygen atom of the catecholate ligand, as corroborated by the following density functional theory (DFT) calculations.

We conducted DFT calculations on the coupling reaction of 1,2-dimethylindole with (*E*)-pent-3-en-2-one as a representative case for the formation of carbazole product **2c**. The calculations were performed at the B3LYP-D3/def2-TZVP//def2-SVP level of theory using the ORCA 4.2.0 software, and computational details are provided in the Supporting Information.[15] In light of the spectroscopic detection of Ru−H species by NMR, we first focused on identifying the catalytically active species and found that the displacement of the benzene ligand from complex **1** (**A0** in the computed model) by the indole substrate is energetically favorable (Figure 2). The formation of 18-electron Ru−H species **A1** was calculated to be downhill by −18.3 kcal/mol in the presence of **L1**, where the redox-active benzoquinone **L1** was added in its reduced catecholate form, substantially increasing the acidity of the Ru−H moiety on **A1**. Proton transfer from the Ru−H bond of **A1** readily proceeds to the nucleophilic C3 position on the indole moiety, and the resulting indolinium of **A2** is isoenergetic with a low barrier of 13.9 kcal/mol. The calculations suggest that the catalytically relevant Ru−H species should have a relatively short lifetime in the presence of a catecholate ligand, which explains why it could not be experimentally detected in the aforementioned NMR study. The subsequent proton transfer from the indole to benzoquinone ligand **L1** proceeds smoothly with a low energy barrier of 9.9 kcal/mol, forming intermediate **A3**.

The Ru-indole-catecholate species **A3** has a vacant coordination site on the Ru center, in which the indole moiety of **A3** effectively serves as a proton shuttle, transferring the hydrogen from the metal center to the oxygen atom of **L1**. The exergonic ligand exchange between the enone and the weakly coordinating indole substrates forms enone-coordinated complex **B1**, which lies at −27.4 kcal/mol relative to **A0**. The relative stability of **B1**, compared to that of **A1′** at −9.8 kcal/mol, underscores the importance of the initial proton transfer steps in facilitating the preactivation of the Ru catalyst. The coupling of the enone moiety in **B1** with the indole substrate is energetically demanding; the electrophilic $\beta$-carbon of the enone undergoes C−C bond formation followed by rotation along the newly forming C−C bond with the indole via **B1-TS**, resulting in the formation of the Ru-indole intermediate **B2** ($\Delta G^{\ddagger}$ = 31.4 kcal/mol). The proton transfer step via **B2-TS** is nearly barrierless, rapidly leading to the formation of Ru-enol species **B3**. The subsequent keto−enol tautomerization of **B3** gives easy access to the keto form of the Ru-indole species **B4**, which is stabilized by both the carbonyl and alkylated indole moieties. The complex **B4** is now set to undergo the key $sp^3$ C−H activation step.

We continued to investigate the reaction mechanism through a combination of experimental and computational methods. First, we examined the electronic effects on decorating the indole substrates with different functional groups. Thus, the reaction rate was measured using NMR spectroscopy for a series of *para*-substituted indoles 5-X-1,2-dimethylindole (0.20 mmol) (X = OMe, Me, H, F, and Cl)

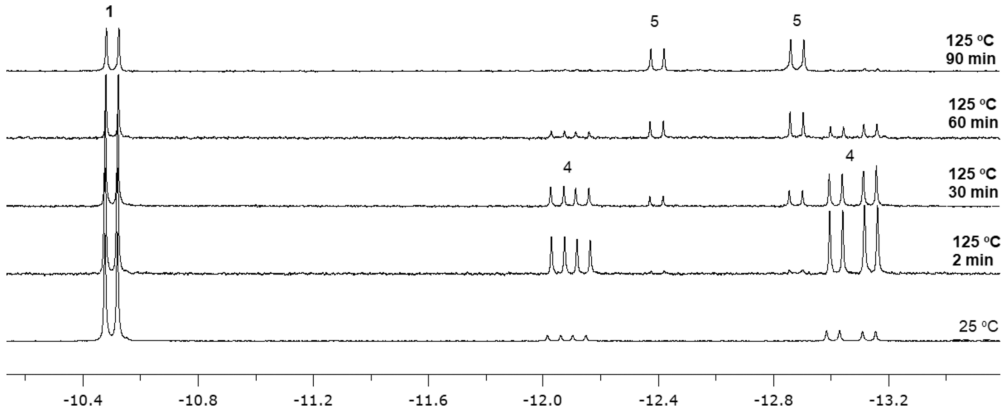


**Figure 1.** Partial $^1$H NMR ($CD_2Cl_2$, 400 MHz) spectra of the reaction of **1** with 1,2-dimethylindole and (*E*)-3-penten-2-one.


https://doi.org/10.1021/acs.organomet.4c00470
Organometallics 2025, 44, 325−334

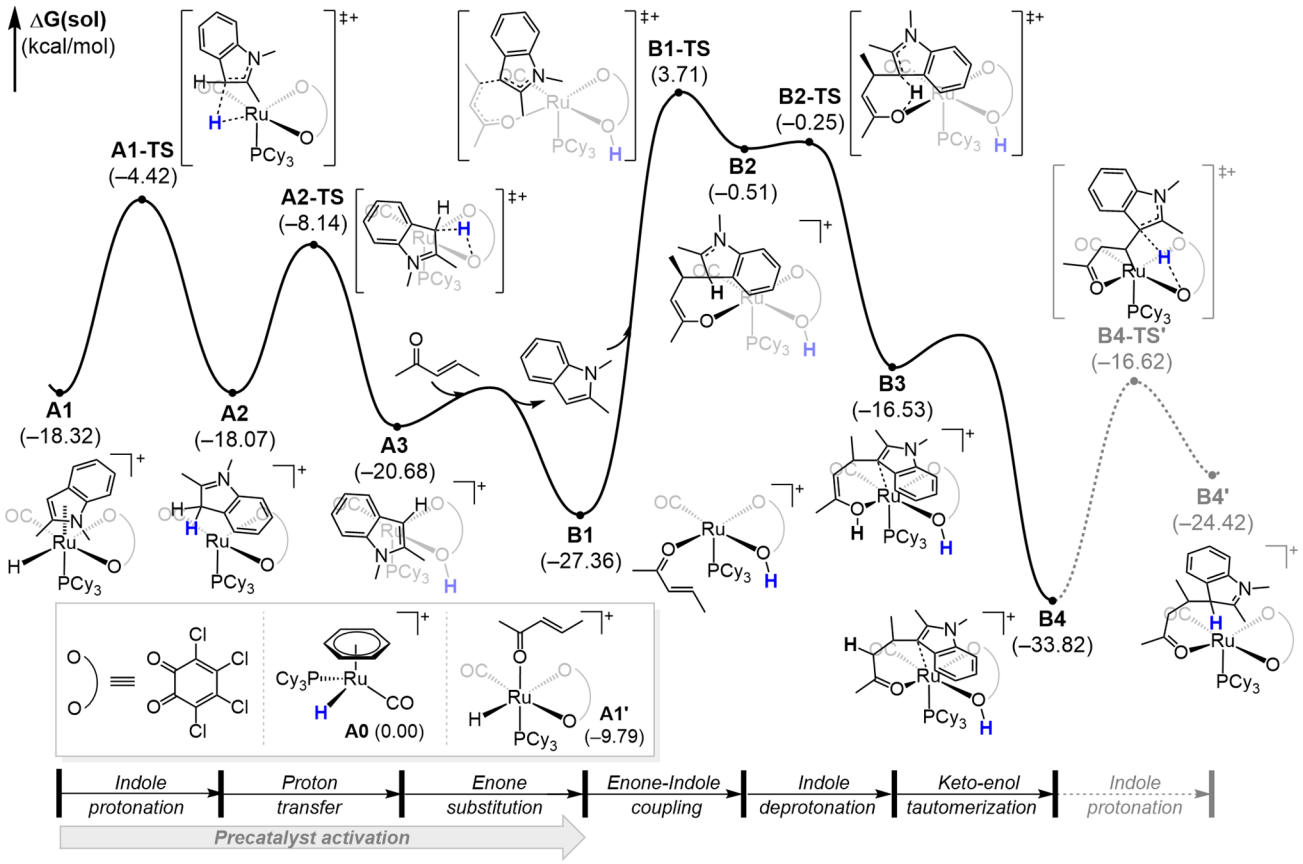


**Figure 2.** Computed energy profile for the precatalyst activation and the alkylation steps for the coupling reaction of 1,2-dimethylindole with (*E*)-pent-3-en-2-one.

with 4-phenyl-3-buten-2-one (0.20 mmol) under standard conditions. The $k_{obs}$ for each reaction was determined from a first-order plot of $-\ln[(1,2\text{-dimethylindole})_t/(1,2\text{-dimethylindole})_0]$ vs time. The Hammett plot of $\log(k_X/k_H)$ vs $\sigma_p$ showed a linear correlation, indicating that the coupling reaction is promoted by an electron-donating group of the indole substrate ($\rho = -1.6 \pm 0.2$) (Figure 3). Strong promotional effect from electron-rich indole substrates implicates a significant buildup of positive charge on the transition state, which is mediated by a cationic Ru catalyst.

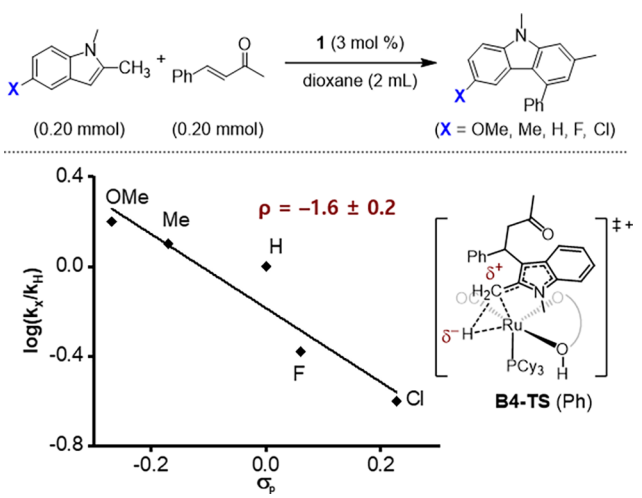


**Figure 3.** Experimental Hammett plot from the reaction of 5-X-1,2-dimethylindole with 4-phenyl-3-buten-2-one (X = OMe, Me, H, F, and Cl).

Since C–H bond activation is frequently the most difficult step in many $sp^3$ C–H functionalization reactions,[16] we measured the deuterium kinetic isotope effect (KIE) to validate the C–H activation as rate-limiting step for the coupling reaction. The reaction rate between 1,2-dimethylindole (0.10 mmol) and 1-methyl-2-(methyl-$d_3$)indole (92% D, 0.10 mmol) with (*E*)-3-penten-2-one in the presence of complex **1** (3 mol %) and *t*-butylethylene (0.10 mmol) in 1,4-dioxane-$d_8$ (1 mL) was independently measured by NMR under a parallel reaction setting (eq 1). The first-order plot of $-\ln[(1,2\text{-dimethylindole})_t/(1,2\text{-dimethylindole})_0]$ vs time showed a normal deuterium isotope effect of $k_H/k_D = 2.5 \pm 0.2$ (Figure S5, Supporting Information). To discern the reversibility of the C–H activation step, we also measured the deuterium KIE under intermolecular competitive conditions. The rate of the coupling reaction of a 1:1 mixture of the presynthesized 4-(1,2-dimethyl-1*H*-indol-3-yl)pentan-2-one and 4-(1-methyl-2-(methyl-$d_3$)-1*H*-indol-3-yl)pentane-2-one under otherwise standard conditions was measured by using the NMR spectroscopic method (eq 2). The first-order plot led to a similar normal deuterium isotope effect of $k_H/k_D = 2.2 \pm 0.2$ (Figure S6, Supporting Information). The observation of a relatively high normal deuterium KIE value under both parallel and competitive conditions supports the notion that the $sp^3$ C–H bond cleavage is the turnover-limiting step for the coupling reaction.[17]

To evaluate reversibility of the C–H activation step, we examined the H/D exchange pattern from the coupling


https://doi.org/10.1021/acs.organomet.4c00470
Organometallics 2025, 44, 325–334

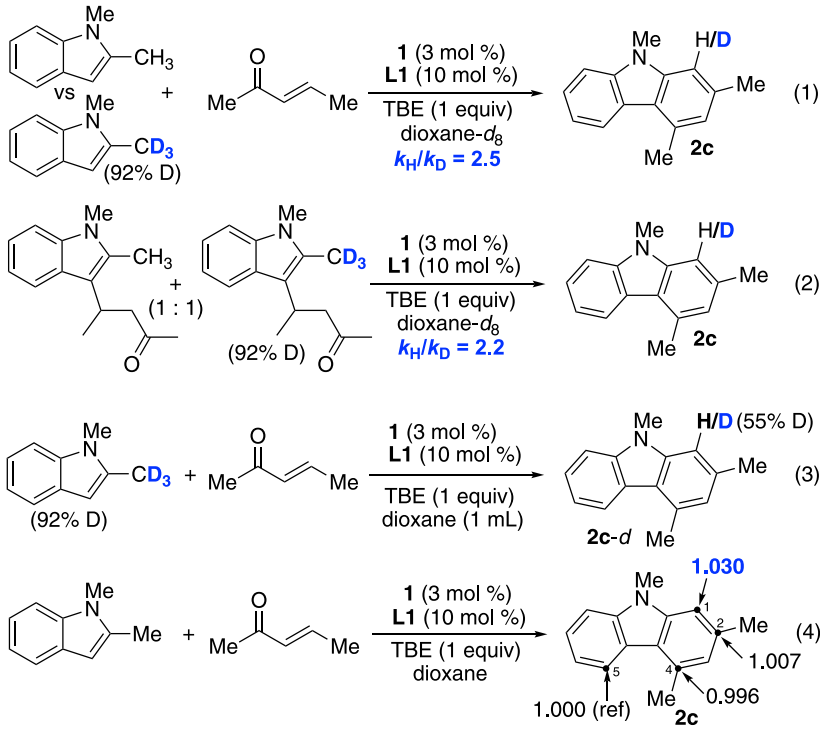


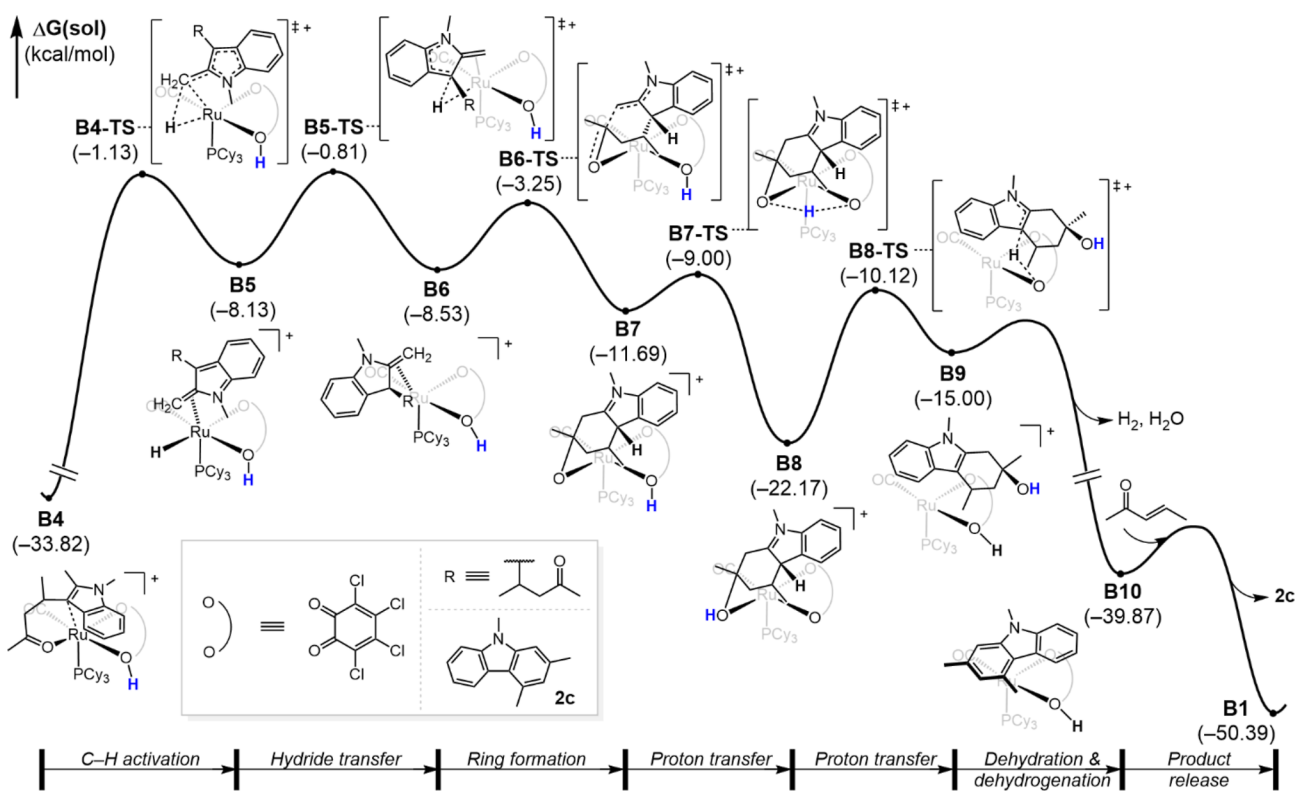


**Figure 4.** Computed energy profile for the C−H activation and the xanthene product **2c** formation steps.

reaction of 1,2-dimethylindole with (*E*)-3-penten-2-one (eq 3). The coupling reaction of 1-methyl-2-(methyl-$d_3$)indole (0.50 mmol) with (*E*)-3-penten-2-one (0.60 mmol) in the presence of complex **1** (3 mol %)/**L1** (10 mol %) and *t*-butylethylene (0.5 mmol) was performed under standard conditions. The isolated product **2c**-*d* showed nearly 55% deuterium on the C(1) arene carbon, as analyzed by both $^1$H and $^2$H NMR spectroscopic methods (Figure S1, Supporting Information). The subsequent control experiments revealed that the H/D exchange process predominantly occurred after the product formation. For instance, the treatment of isolated **2c** with $D_2O$ (2 equiv) under the standard conditions resulted in an extensive deuterium incorporation at both the C(1) and C(3) arene positions of **2c** (Figure S2, Supporting Information). The results suggest that the sp$^3$ C−H activation is a largely irreversible process and that the observed deuterium labeling


https://doi.org/10.1021/acs.organomet.4c00470
Organometallics 2025, 44, 325−334

**Scheme 3. Proposed Mechanism of the Formation of Carbazole Product 2 from the Dehydrative sp$^3$ C−H Coupling Reaction of 1,2-Dimethylindole with an Enone**

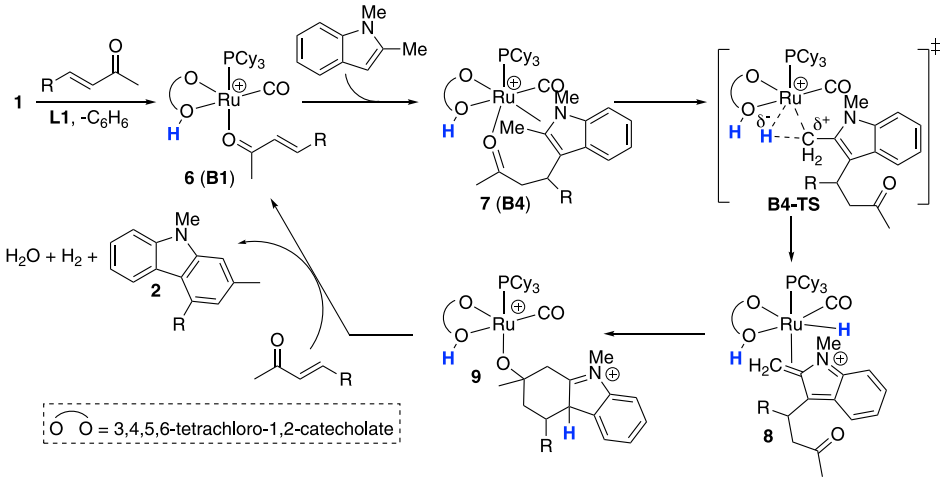


pattern on the methyl position of **2c** was primarily resulted from the H/D exchange with the byproduct $D_2O$.

To further ascertain rate-limiting step of the coupling reaction, we measured the carbon KIE of the coupling reaction by using Singleton's NMR technique at natural abundance.[18] The reaction mixture of 1,2-dimethylindole (0.5 mmol), (*E*)-3-penten-2-one (0.6 mmol), and *t*-butylethylene (0.5 mmol) in the presence of **1** (3 mol %) and **L1** (10 mol %) in 1,4-dioxane (2 mL) was heated at 135 °C for 24 h (eq 4). A high conversion sample of product **2c** was isolated by column chromatography on silica gel, and the procedure was repeated two more times. The same experimental procedure was used to obtain a low conversion sample of product **2c** by stopping the reaction after 2 h. The carbon KIE was measured by comparing the ratio of $^{13}C$ incorporation ($^{13}C$ (avg 80% conversion)/$^{13}C$ (avg 15% conversion)) by using the high precision $^{13}C\{^1H\}$ NMR analysis technique. The most significant carbon KIE was observed on the C(1) arene carbon of product **2c**. While the carbon KIE result can be interpreted by either sp$^3$ C−H bond activation or C−C bond formation as the slow step, the combined carbon and deuterium KIE results are more consistent with the sp$^3$ C−H bond activation as the rate-determining step for the coupling reaction.

To corroborate these experimental results, we continued the DFT calculations on the coupling reaction, and the complete reaction profile is illustrated in Figure 4. Our computer simulations confirmed that the sp$^3$ C−H bond activation step from **B4** to **B5** has a high barrier ($\Delta G^{\ddagger}$ = 32.7 kcal/mol) traversing **B4-TS**, which lies at −1.1 kcal/mol relative to **A0**. Such a high barrier is certainly consistent with the experimental deuterium KIE data, where a normal KIE of $k_H/k_D$ = 2.5 was measured at an elevated temperature of 135 °C. In examining **B4-TS** more closely, we found that the highly electrophilic Ru(II) center facilitates the cleavage of C−H bond heterolytically rather than in a classical oxidative addition mechanism. The resonance stabilization of the resulting iminium-indole species **B5** further supports the heterolytic C−H cleavage mechanism, which is also corroborated by the observation of a negative slope in the Hammett correlation as illustrated in Figure 3 that signifies a buildup of positive charge in the transition state. We also considered an alternate C−H activation mechanism via the formation of a protonated indole **B4′**, but this pathway was found to be much less favorable than the pathway via **B4-TS** in the later stages of the reaction path (Figure S9, Supporting Information). In addition, the putative intermediate **B4′** is favored to lose the indole moiety in the presence of 2-propanol (under a hydrogen-rich condition), which channels into the reaction path for the formation of C−C bond cleavage product **3** instead of undergoing the C−H activation path to afford the carbazole product **2** (vide infra).

While the energies of **B4-TS** and **B5-TS** are nearly identical, the experimentally determined deuterium KIE and the Hammett data support that the conversion of **B4** to **B5** via **B4-TS** is most likely the rate-determining step of the coupling reaction. The hydride transfer to the C3 position of the indole in **B5** readily proceeds with a relatively small barrier of 7.3 kcal/mol via **B5-TS** to form **B6**. The subsequent cyclization and the C−C bond formation between the carbonyl carbon and C2 carbon of the indole via **B6-TS** leads to the Ru-alkoxy species **B7**. This C−C bond formation process is expected to be quite facile with a low barrier of $\Delta G^{\ddagger}$ = 5.3 kcal/mol. The catecholate ligand **L1** of cyclized intermediate **B7** promotes two consecutive proton transfers via **B7-TS** and **B8-TS** to form intermediate **B9**. The subsequent dehydrogenation and dehydration steps are highly exergonic ($\Delta G$ = −23.0 kcal/mol), providing the thermodynamic driving force for the formation of carbazole product **2c** along with an irreversible release of the $H_2$ byproduct.

To discern the factors guiding the selective formation of carbazole product **2** over the C−C cleavage product **3**, we performed the DFT calculations on the intermediate **B4′** with 2-propanol under a hydrogen-rich condition (Figure S10, Supporting Information). In the presence of 2-propanol, complex **B4′** bearing protonated indole undergoes a facile dissociation of the indole to form a free iminium-indole upon the addition of a 2-propanol molecule ($\Delta G^{\ddagger}$ = 7.0 kcal/mol). The protonated iminium-indole readily undergoes an organic C−C cleavage reaction with a barrier of 20.3 kcal/mol on the C−C cleavage step. The dissociation of the alkylated indole is crucial in providing a vacant site for the activation of 2-propanol molecule, which delivers entropic benefits for the C−C bond cleavage step (Figure S11, Supporting Information). The resulting iminium intermediate **int3** eventually recoordinates to the Ru center, and the product **3c** is released after accepting a hydride from the Ru catalyst. The DFT calculation results are consistent with the experimental observation that


https://doi.org/10.1021/acs.organomet.4c00470
Organometallics 2025, 44, 325−334

catalyst **1** without **L1** still formed **2a** but with a significantly lower yield (Table 1, entry 3) because the key intermediate **B4** without catechol ligand should favor the C−C cleavage pathway in forming **3c**. Overall, the formation of compound **3c** is accompanied by the release of two acetone molecules. Since acetone has a relatively low boiling point (b.p. = 56 °C), it is unlikely to participate in the reverse reaction, providing the driving force for the formation of **3c**. Detailed computed C−C cleavage reaction path and the formation of **3c** are compiled in the Supporting Information.

**Proposed Mechanism.** We compiled a detailed mechanism of the formation of carbazole product **2**, by combining our experimental and computational explorations into the mechanism (Scheme 3). We propose that the catalytically active Ru-catecholate-hydride species **6** (**B1**) is initially formed from the precatalyst **1** (**A0**) after undergoing a series of ligand displacements and reductive coordination of the benzoquinone ligand **L1**. In support of the formation of the Ru-catecholate complex, we previously synthesized a similar Ru-catecholate complex from the reaction of the Ru−H complex with a 1,2-catechol ligand.[12] As illustrated in Scheme 2, we have detected both indole- and carbazole-coordinated Ru−H species **4** and **5** from the reaction of **1** with indole and enone substrates. The DFT calculations established a plausible precatalyst activation mechanism via sequential ligand displacement and rearrangement that lead to the formation of a stable Ru-catecholate-hydride complex **6** (**B1**) with an enone substrate. The conjugate addition of the indole substrate to the coordinated enone of **6** should form the elaborated Ru-indole complex **7** (**B4**). The DFT calculations showed that energetically demanding C−C bond formation is facilitated by an electrophilic Ru catalyst. Directed by the carbonyl group, the intermediate **7** promotes the key $sp^3$ C−H activation step of the elaborated indole moiety. Furthermore, the calculations revealed that the electrophilic nature of the ruthenium center facilitates the $sp^3$ C−H activation in a heterolytic process via the transition state **B4-TS** rather than the classical oxidative addition mechanism in forming the iminium-ion-coordinated Ru−H complex **8**. A relatively high normal deuterium KIE ($k_H/k_D$ = 2.5) and the Hammett correlation data ($\rho$ = −1.6) also support the notion that the heterolytic C−H bond cleavage is the rate-limiting step for the coupling reaction. In addition, a buildup of the positive charge advocates the formation of an iminium-indole, which makes the heterolytic C−H cleavage plausible. The calculations provided a reasonable pathway for the formation of the carbazole product **2** that the catecholate ligand of the Ru-iminium-indole complex **8** facilitates the cyclization (C−C bond formation) by promoting a series of rapid proton transfer steps to give the Ru-alkoxy species **9**. A highly exergonic dehydration and the subsequent aromatization steps are driven by the irreversible release of water and $H_2$, both of which provide the thermodynamic driving force for the formation of the carbazole product **2** with the regeneration of the Ru−H species **6**. The DFT calculations also established a plausible mechanism for the formation of the C−C cleavage product **3**, where the indole complex **7** (**B4**) prefers to undergo a proton transfer to the indole in the presence of 2-propanol (under a hydrogen-rich condition) to form a new elaborated complex **B4′**. The resulting indolinium moiety of **B4′** has been found to be much more susceptible to the ligand displacement reaction by 2-propanol. The free indolinium ion would proceed with a series of organic hydrogenolysis and rearrangement steps under the thermal reaction conditions to form C−C cleavage product **3**.

Both the DFT calculation and Hammett correlation data provided compelling evidence for a heterolytic $sp^3$ C−H cleavage mechanism by the Ru catalytic system **1**/**L1**. Transition metal-mediated heterolytic C−H bond cleavage processes have long been known to be a prominent C−H activation mode in a number of industrially significant dehydrogenation and related hydrocarbon feedstock reforming processes mediated by heterogeneous metal oxide catalysts.[19] In contrast, heterolytic C−H bond cleavage mechanisms have been rarely observed, especially in catalytic $sp^3$ C−H bond functionalization reactions mediated by soluble transition metal complexes. While both early and late transition metal complexes bearing heteroatom-containing ligands have been known to promote heterolytic sp and $sp^2$ C−H bond cleavage reactions under stoichiometric reaction settings,[20] catalytic C−H functionalization reactions via heterolytic $sp^3$ C−H cleavage for saturated hydrocarbon substrates are exceedingly rare. In seminal examples, Legzdin and Mindiola groups reported that heterolytic cleavage of $sp^2$ arene C−H bonds is readily mediated by early transition metal-carbene complexes.[21] Recently, Nozaki and co-workers reported a stoichiometric reductive elimination reaction of a Pt(IV)-methyl complex, in which the heterolytic $sp^3$ C−H bond cleavage process is facilitated by a metal−ligand cooperative function.[22] Daugulis proposed a heterolytic $sp^2$ arene C−H cleavage mechanism in Pd-catalyzed *ortho*-arene C−H arylation of benzoic acid derivatives.[23] In our case, the Ru-catecholate catalyst system has a unique ability to promote metal−ligand cooperative activity between an electrophilic Ru center and the catecholate ligand for facilitating a series of proton transfer steps, which, in turn, leads to heterolytic $sp^3$ C−H bond cleavage of the 2-alkylindole substrate. We are currently exploring the heterolytic $sp^3$ C−H bond cleavage mode of activity of our Ru catalyst toward promoting the C−C coupling reactions of other saturated hydrocarbon substrates bearing heteroatom functional groups.

## CONCLUSIONS

In summary, we have successfully developed a new catalytic dehydrative $sp^3$ C−H coupling reaction of indoles with enones as an efficient synthetic protocol for carbazole derivatives. The catalytic coupling method provides a convergent synthetic protocol for 2,4-disubstituted carbazole derivatives without using reactive reagents that are otherwise difficult to achieve from other traditional synthetic methods. We have compiled a detailed mechanistic picture of the catalytic reaction from combined experimental and computational studies, which features an initial conjugate addition of the indole substrate, followed by a series of C−H activation, cyclization, dehydration, and aromatization steps. The mechanistic study further revealed that the synergistic metal−ligand cooperative activity between the electrophilic Ru center and the catecholate ligand plays a critical role in facilitating the heterolytic $sp^3$ C−H activation process and the formation of the carbazole products. Studies toward exploiting the heterolytic C−H cleavage process in other catalytic C−C coupling reactions of saturated hydrocarbon substrates are currently being pursued in our laboratory.


https://doi.org/10.1021/acs.organomet.4c00470
Organometallics 2025, 44, 325−334

## EXPERIMENTAL SECTION

**General Procedure for the Coupling Reaction of 1,2-Dimethylindole with an Enone.** In a glovebox, 1,2-dimethylindole (0.50 mmol), an enone (0.60 mmol), TBE (0.50 mmol), complex **1** (3 mol %), and **L1** (10 mol %) were dissolved in anhydrous 1,4-dioxane (2 mL) in a 25 mL Schlenk tube equipped with a Teflon stopcock and a magnetic stirring bar. The tube was brought out of the glovebox and was stirred in an oil bath set at 135 °C for 24 h. The reaction tube was taken out of the oil bath and was cooled to room temperature. After the tube was open to air, the solution was filtered through a short silica gel column by eluting with $CH_2Cl_2$ (10 mL), and the filtrate was analyzed by GC-MS. The analytically pure product was isolated by column chromatography on silica gel (40−63 μm particle size, hexanes/EtOAc). The product was completely characterized by NMR and GC-MS spectroscopic methods.

**General DFT Computational Procedure.** All DFT calculations were performed with the ORCA 4.2.0 program.[15] Electronic exchange and correlation energy contributions to the total electronic energy were approximated with the B3LYP hybrid exchange functional along with Grimme's D3 dispersion correction (B3LYP-D3).[24] All intermediate and transition state geometries were optimized with the def2-SVP basis set for main group atoms and the def2-ECP basis set for Ru.[25,26] While these basis sets are adequate for obtaining accurate geometries, more reliable energies were obtained from the single point calculations using the Karlsruhe triple-ζ basis set, def2-TZVP for main group atoms and the def2-ECP basis set for Ru.[25,26] The zero-point energy, thermal energy, and entropic and solvation contributions to the Gibbs energy are obtained from the same level of theory used in the geometry optimizations (B3LYP-D3/def2-SVP/def2-ECP(Ru)). The optimized geometries characterized as the local minima on the potential energy surfaces do not contain any imaginary frequencies, whereas each transition state contains one imaginary frequency. The solution environment for 1,4-dioxane was modeled with the conductor-like polarizable continuum model (C-PCM) method with a dielectric constant of 2.209 and refractive index of 1.4224.[27]

## ASSOCIATED CONTENT

### Supporting Information

The Supporting Information is available free of charge at https://pubs.acs.org/doi/10.1021/acs.organomet.4c00470.

Experimental procedures, characterization data, NMR spectra for organic products, and computational details (PDF)

Structures of optimized geometries (XYZ)

### Accession Codes

Deposition Number 2377617 contains the supplementary crystallographic data for this paper. These data can be obtained free of charge via the joint Cambridge Crystallographic Data Centre (CCDC) and Fachinformationszentrum Karlsruhe Access Structures service.

## AUTHOR INFORMATION


### Corresponding Authors

**Mu-Hyun Baik** − *Center for Catalytic Hydrocarbon Functionalizations, Institute for Basic Science (IBS), Daejeon 34141, Republic of Korea; Department of Chemistry, Korea Advanced Institute of Science and Technology (KAIST), Daejeon 34141, Republic of Korea;* orcid.org/0000-0002-8832-8187; Email: mbaik2805@kaist.ac.kr

**Chae S. Yi** − *Department of Chemistry, Marquette University, Milwaukee, Wisconsin 53233, United States;* orcid.org/0000-0002-4504-1151; Email: chae.yi@marquette.edu

### Authors

**Krishna Prasad Gnyawali** − *Department of Chemistry, Marquette University, Milwaukee, Wisconsin 53233, United States*

**Mina Son** − *Department of Chemistry, Korea Advanced Institute of Science and Technology (KAIST), Daejeon 34141, Republic of Korea; Center for Catalytic Hydrocarbon Functionalizations, Institute for Basic Science (IBS), Daejeon 34141, Republic of Korea;* orcid.org/0000-0001-5689-1648

**Donghun Hwang** − *Department of Chemistry, Korea Advanced Institute of Science and Technology (KAIST), Daejeon 34141, Republic of Korea; Center for Catalytic Hydrocarbon Functionalizations, Institute for Basic Science (IBS), Daejeon 34141, Republic of Korea;* orcid.org/0009-0007-4451-8433

**Nuwan Pannilawithana** − *Department of Chemistry, Marquette University, Milwaukee, Wisconsin 53233, United States;* orcid.org/0000-0003-0148-7781

Complete contact information is available at: https://pubs.acs.org/10.1021/acs.organomet.4c00470


### Notes

The authors declare no competing financial interest.

## ACKNOWLEDGMENTS

Financial support from the National Science Foundation (CHE-2153885) is gratefully acknowledged. C.S.Y. acknowledges 2022 Way-Klinger Fellowship Award (Marquette University), and M.-H.B. acknowledges financial support from the Institute for Basic Science in Korea (IBS-R010-A1).

## REFERENCES


(1) Recent reviews (a) Bellina, F.; Rossi, R. Transition Metal-Catalyzed Direct Arylation of Substrates with Activated $sp^3$-Hybridized C−H Bonds and Some of Their Synthetic Equivalents with Aryl Halides and Pseudohalides. *Chem. Rev.* **2010**, *110*, 1082−1146. (b) He, J.; Wasa, M.; Chan, K. S. L.; Shao, Q.; Yu, J.-Q. Palladium-Catalyzed Transformations of Alkyl C−H Bonds. *Chem. Rev.* **2017**, *117*, 8754−8786. (c) Sinha, S. K.; Guin, S.; Maiti, S.; Biswas, J. P.; Porey, S.; Maiti, D. Toolbox for Distal C−H Bond Functionalizations in Organic Molecules. *Chem. Rev.* **2022**, *122*, 5682−5841.

(2) Yamaguchi, J.; Yamaguchi, A. D.; Itami, K. C−H Bond Functionalization: Emerging Synthetic Tools for Natural Products and Pharmaceuticals. *Angew. Chem., Int. Ed.* **2012**, *51*, 8960−9009.

(3) (a) Huang, Z.; Lim, H. N.; Mo, F.; Young, M. C.; Dong, G. Transition-metal catalyzed ketone-directed or mediated C−H functionalization. *Chem. Soc. Rev.* **2015**, *44*, 7764−7786. (b) Dong, Z.; Ren, Z.; Thompson, S. J.; Xu, Y.; Dong, G. Transition-Metal-Catalyzed C−H Alkylation Using Alkenes. *Chem. Rev.* **2017**, *117*, 9333−9403. (c) Chen, Z.; Rong, M.-Y.; Nie, J.; Zhu, X.-F.; Shi, B.-F.; Ma, J.-A. Catalytic alkylation of unactivated $C(sp^3)$−H bonds for $C(sp^3)$−$C(sp^3)$ bond formation. *Chem. Soc. Rev.* **2019**, *48*, 4921−4942.

(4) (a) Park, Y. J.; Park, J.-W.; Jun, C.-H. Metal-Organic Cooperative Catalysis in C−H and C−C Bond Activation and Its Concurrent Recovery. *Acc. Chem. Res.* **2008**, *41*, 222−234. (b) Kim, D.-S.; Park, W.-J.; Jun, C.-H. Metal−Organic Cooperative Catalysis in C−H and C−C Bond Activation. *Chem. Rev.* **2017**, *117*, 8977−9015.

(5) He, G.; Wang, B.; Nack, W. A.; Chen, G. Syntheses and Transformations of α-Amino Acids via Palladium-Catalyzed Auxiliary-Directed $sp^3$ C−H Functionalization. *Acc. Chem. Res.* **2016**, *49*, 635−645.

(6) (a) Li, Z.; Bohle, D. S.; Li, C.-J. Cu-catalyzed cross-dehydrogenative coupling: a versatile strategy for C−C bond formations via the oxidative activation of $sp^3$ C−H bonds. *Proc. Natl. Acad. Sci. U.S.A.* **2006**, *103*, 8928−8933. (b) Yeung, C. S.; Dong, V. M. Catalytic Dehydrogenative Cross-Coupling: Forming Carbon-Carbon Bonds by Oxidizing Two Carbon-Hydrogen Bonds. *Chem. Rev.* **2011**, *111*, 1215−1292. (c) Huang, C.-Y.; Kang, H.; Li, J.; Li, C.-J. En Route to Intermolecular Cross-Dehydrogenative Coupling Reactions. *J. Org. Chem.* **2019**, *84*, 12705−12721.

(7) (a) Wencel-Delord, J.; Glorius, F. C−H bond activation enables the rapid construction and late-stage diversification of functional molecules. *Nat. Chem.* **2013**, *5*, 369. (b) Mo, F.; Dong, G. Regioselective Ketone $\alpha$-Alkylation with Simple Olefins via Dual Activation. *Science* **2014**, *345*, 68−72. (c) Abrams, D. J.; Provencher, P. A.; Sorensen, E. J. Recent applications of C−H functionalization in complex natural product synthesis. *Chem. Soc. Rev.* **2018**, *47*, 8925−8967.

(8) Lucas, E. L.; Lam, N. Y. S.; Zhuang, Z.; Chan, H. S. S.; Strassfeld, D. A.; Yu, J.-Q. Palladium-Catalyzed Enantioselective $\beta$-C($sp^3$)−H Activation Reactions of Aliphatic Acids: A Retrosynthetic Surrogate for Enolate Alkylation and Conjugate Addition. *Acc. Chem. Res.* **2022**, *55*, 537−550.

(9) Capaldo, L.; Ravelli, D.; Fagnoni, M. Direct Photocatalyzed Hydrogen Atom Transfer (HAT) for Aliphatic C−H Bonds Elaboration. *Chem. Rev.* **2022**, *122*, 1875−1924.

(10) Holmberg-Douglas, N.; Nicewicz, D. A. Photoredox-Catalyzed C−H Functionalization Reactions. *Chem. Rev.* **2022**, *122*, 1925−2016.

(11) (a) Lee, D.-H.; Kwon, K.-H.; Yi, C. S. Dehydrative C−H Alkylation and Alkenylation of Phenols with Alcohols: Expedient Synthesis for Substituted Phenols and Benzofurans. *J. Am. Chem. Soc.* **2012**, *134*, 7325−7328. (b) Pannilawithana, N.; Pudasaini, B.; Baik, M.-H.; Yi, C. S. Experimental and Computational Studies on the Ruthenium-Catalyzed Dehydrative C−H Coupling of Phenols with Aldehydes for the Synthesis of 2-Alkylphenol, Benzofuran and Xanthene Derivatives. *J. Am. Chem. Soc.* **2021**, *143*, 13428−13440.

(12) Pannilawithana, N.; Yi, C. S. Catalytic Carbon−Carbon Bond Activation of Saturated and Unsaturated Carbonyl Compounds via Chelate-Assisted Coupling Reaction with Indoles. *ACS Catal.* **2020**, *10*, 5852−5861.

(13) Arachchige, P. T. K.; Handunneththige, S.; Talipov, M. R.; Kalutharage, N.; Yi, C. S. Scope and Mechanism of the Redox-Active 1,2-Benzoquinone Enabled Ruthenium-Catalyzed Deaminative $\alpha$-Alkylation of Ketones with Amines. *ACS Catal.* **2021**, *11*, 13962−13972.

(14) Thennakoon, D. S.; Talipov, M. R.; Yi, C. S. Scope and Mechanism of the Ruthenium Catalyzed Deaminative Coupling Reaction of Enones with Amines via Regioselective $C_\alpha$−$C_\beta$ Bond Cleavage. *Organometallics* **2023**, *42*, 2867−2880.

(15) (a) Neese, F. The ORCA Program System. *Wiley Interdiscip. Rev. Comput. Mol. Sci.* **2012**, *2*, 73−78. (b) Neese, F. Software Update: The ORCA Program System, Version 4.0. *Wiley Interdiscip. Rev.: Comput. Mol. Sci.* **2017**, *8*, No. e1327. (c) Neese, F.; Wennmohs, F.; Becker, U.; Riplinger, C. The ORCA Quantum Chemistry Program Package. *J. Chem. Phys.* **2020**, *152*, 224108.

(16) Recent reviews: (a) Rouquet, G.; Chatani, N. Catalytic Functionalization of C($sp^2$)−H and C($sp^3$)−H Bonds by Using Bidentate Directing Groups. *Angew. Chem., Int. Ed.* **2013**, *52*, 11726−11743. (b) Davies, D. L.; Macgregor, S. A.; McMullin, C. L. Computational Studies of Carboxylate-Assisted C−H Activation and Functionalization at Group 8−10 Transition Metal Centers. *Chem. Rev.* **2017**, *117*, 8649−8709. (c) Liu, B.; Romine, A. M.; Rubel, C. Z.; Engle, K. M.; Shi, B.-F. Transition-Metal-Catalyzed, Coordination-Assisted Functionalization of Nonactivated C($sp^3$)−H Bonds. *Chem. Rev.* **2021**, *121*, 14957−15074.

(17) Simmons, E. M.; Hartwig, J. F. On the Interpretation of Deuterium Kinetic Isotope Effects in C-H Bond Functionalizations by Transition-Metal Complexes. *Angew. Chem., Int. Ed.* **2012**, *51*, 3066−3072.

(18) (a) Singleton, D. A.; Thomas, A. A. High-Precision Simultaneous Determination of Multiple Small Kinetic Isotope Effects at Natural Abundance. *J. Am. Chem. Soc.* **1995**, *117*, 9357−9358. (b) Frantz, D. E.; Singleton, D. A.; Snyder, J. P. $^{13}$C Kinetic Isotope Effects for the Addition of Lithium Dibutylcuprate to Cyclohexenone. Reductive Elimination is Rate-Determining. *J. Am. Chem. Soc.* **1997**, *119*, 3383−3384. (c) Nowlan, D. T.; Gregg, T. M.; Davies, H. M. L.; Singleton, D. A. Isotope Effects and the Nature of Selectivity in Rhodium-Catalyzed Cyclopropanations. *J. Am. Chem. Soc.* **2003**, *125*, 15902−15911.

(19) (a) Sloan, E. D., Jr. Fundamental principles and applications of natural gas hydrates. *Nature* **2003**, *426*, 353−359. (b) Sattler, J. J. H. B.; Ruiz-Martinez, J.; Santillan-Jimenez, E.; Weckhuysen, B. M. Catalytic Dehydrogenation of Light Alkanes on Metals and Metal Oxides. *Chem. Rev.* **2014**, *114*, 10613−10653.

(20) Higashi, T.; Kusumoto, S.; Nozaki, K. Cleavage of Si−H, B−H, and C−H Bonds by Metal-Ligand Cooperation. *Chem. Rev.* **2019**, *119*, 10393−10402.

(21) (a) Pamplin, C. B.; Legzdins, P. Thermal Activation of Hydrocarbon C−H Bonds by Cp*M(NO) Complexes of Molybdenum and Tungsten. *Acc. Chem. Res.* **2003**, *36*, 223−233. (b) Bailey, B. C.; Fan, H.; Baum, E. W.; Huffman, J. C.; Baik, M.-H.; Mindiola, D. J. Intermolecular C−H Bond Activation Promoted by a Titanium Alkylidyne. *J. Am. Chem. Soc.* **2005**, *127*, 16016−16017.

(22) Higashi, T.; Ando, H.; Kusumoto, S.; Nozaki, K. Metal-Ligand Cooperative C−H Bond Formation by Cyclopentadienone Platinum Complexes. *J. Am. Chem. Soc.* **2019**, *141*, 2247−2250.

(23) Chiong, H. A.; Pham, Q.-N.; Daugulis, O. Two Methods for Direct *ortho*-Arylation of Benzoic Acids. *J. Am. Chem. Soc.* **2007**, *129*, 9879−9884.

(24) (a) Becke, A. D. Density-Functional Exchange-Energy Approximation with Correct Asymptotic Behavior. *Phys. Rev. A* **1988**, *38*, 3098−3100. (b) Lee, C.; Yang, W.; Parr, R. G. Development of the Colle-Salvetti Correlation-Energy Formula into a Functional of the Electron Density. *Phys. Rev. B* **1988**, *37*, 785−789. (c) Grimme, S.; Antony, J.; Ehrlich, S.; Krieg, H. A Consistent and Accurate Ab Initio Parametrization of Density Functional Dispersion Correction (DFT-D) for the 94 Elements H-Pu. *J. Chem. Phys.* **2010**, *132*, 154104.

(25) (a) Schäfer, A.; Horn, H.; Ahlrichs, R. Fully Optimized Contracted Gaussian Basis Sets for Atoms Li to Kr. *J. Chem. Phys.* **1992**, *97*, 2571−2577. (b) Schäfer, A.; Huber, C.; Ahlrichs, R. Fully Optimized Contracted Gaussian Basis Sets of Triple Zeta Valence Quality for Atoms Li to Kr. *J. Chem. Phys.* **1994**, *100*, 5829−5835. (c) Weigend, F.; Ahlrichs, R. Balanced Basis Sets of Split Valence, Triple Zeta Valence and Quadruple Zeta Valence Quality for H to Rn: Design and Assessment of Accuracy. *Phys. Chem. Chem. Phys.* **2005**, *7*, 3297−3305. (d) Weigend, F. Accurate Coulomb-Fitting Basis Sets for H to Rn. *Phys. Chem. Chem. Phys.* **2006**, *8*, 1057−1065.

(26) Andrae, D.; Häußermann, U.; Dolg, M.; Stoll, H.; Preuß, H. Energy-Adjusted Ab Initio Pseudopotentials for the Second and Third Row Transition Elements. *Theor. Chim. Acta* **1990**, *77*, 123−141.

(27) Barone, V.; Cossi, M. Quantum Calculation of Molecular Energies and Energy Gradients in Solution by a Conductor Solvent Model. *J. Phys. Chem. A* **1998**, *102*, 1995−2001.



https://doi.org/10.1021/acs.organomet.4c00470
*Organometallics* 2025, 44, 325−334